RSC Advances

PAPER

View Article Online
View Journal | View Issue

Cite this: *RSC Adv.*, 2022, **12**, 26220

Main-chain flexibility and hydrophobicity of ionenes strongly impact their antimicrobial activity: an extended study on drug resistance strains and *Mycobacterium*†

Rafał Jerzy Kopiasz,[a] Anna Zabost,[b] Magdalena Myszka,[a] Aleksandra Kuźmińska,[c] Karolina Drężek,[a] Jolanta Mierzejewska,[a] Waldemar Tomaszewski,[a] Agnieszka Iwańska,[b] Ewa Augustynowicz-Kopeć,[b] Tomasz Ciach[c] and Dominik Jańczewski[a]

The spread of antibiotic-resistant pathogens and the resurgence of tuberculosis disease are major motivations to search for novel antimicrobial agents. Some promising candidates in this respect are cationic polymers, also known as synthetic mimics of antimicrobial peptides (SMAMPs), which act through the membrane-lytic mechanism. Development of resistance toward SMAMPs is less likely than toward currently employed antibiotics; however, further studies are needed to better understand their structure–activity relationship. The main objective of this work is to understand the cross-influence of hydrophobicity, main-chain flexibility, and the topology of ionenes (polycations containing a cationic moiety within the main-chain) on activity. To fulfill this goal, a library of ionenes was developed and compared with previously investigated molecules. The obtained compounds display promising activity against the model microorganisms and drug-resistance clinical isolates, including *Mycobacterium tuberculosis*. The killing efficiency was also investigated, and results confirm a strong effect of hydrophobicity, revealing higher activity for molecules possessing the flexible linker within the polymer main-chain.

Received 4th July 2022
Accepted 30th August 2022

DOI: 10.1039/d2ra04121a

rsc.li/rsc-advances

1. Introduction

The spread of antibiotic resistance among pathogens is a serious concern to the global healthcare and economy.[1,2] One of the pathogens responsible for the highest mortality worldwide is *Mycobacterium tuberculosis* (*Mtb*), the causative agent of tuberculosis disease (TB). Humanity has been relatively successful in the limitation of TB in the last 100 years, however, the increasing number of rifampicin-resistant TB (RS-TB) and multidrug-resistant TB (MDR-TB) cases has led to the reemergence of this illness. In 2019, it was estimated that 10 million people fell ill with TB, about 1.2 million died due to TB, and almost half a million people developed RS-TB, of which 78% had MDR-TB.[3,4] To avoid a global health crisis caused by highly infective drug-resistant bacteria, a strong effort to develop novel antibacterial agents is urgently needed.[5] Unfortunately, there is an alarming scarcity of new antibiotics in the market.[1] The high cost of research combined with a relatively low financial return, makes new antibiotic research not profitable enough for pharmaceutical companies.[6–8] Therefore, academic studies in this area are critical.

Membrane lytic compounds, such as antimicrobial peptides (AMPs)[9,10] and their synthetic mimics (SMAMPs), are a promising class of antimicrobials. There are experimental evidences that SMAMPs display lower susceptibility to the resistance development than currently used antibiotics.[11–13] Due to the more accessible and cheaper synthesis of SMAMPs and easy access to various chemical structures, these compounds seem to outperform AMPs to some extent. SMAMPs are characterized by the presence of positively charged and hydrophobic moieties and an overall amphiphilic character. These features facilitate the initial electrostatic interactions with a negatively charged cell membrane, and subsequent incorporation into a hydrophobic interior of the lipid bilayer, which leads to the membrane disruption and eventually cell death.[14,15] According to the existing theory, a random coil conformation of a moderately hydrophobic amphiphilic polycation turns into globally amphiphilic upon contact with a cell membrane, which allows

[a]*Faculty of Chemistry, Warsaw University of Technology, Noakowskiego 3, Warsaw 00-664, Poland. E-mail: dominik.janczewski@pw.edu.pl*

[b]*Department of Microbiology, National Tuberculosis and Lung Diseases Research Institute, Płocka 26, Warsaw 01-138, Poland*

[c]*Faculty of Chemical and Process Engineering, Warsaw University of Technology, Waryńskiego 1, Warsaw 00-645, Poland*

† Electronic supplementary information (ESI) available: NMR spectra, synthetic scheme. See https://doi.org/10.1039/d2ra04121a

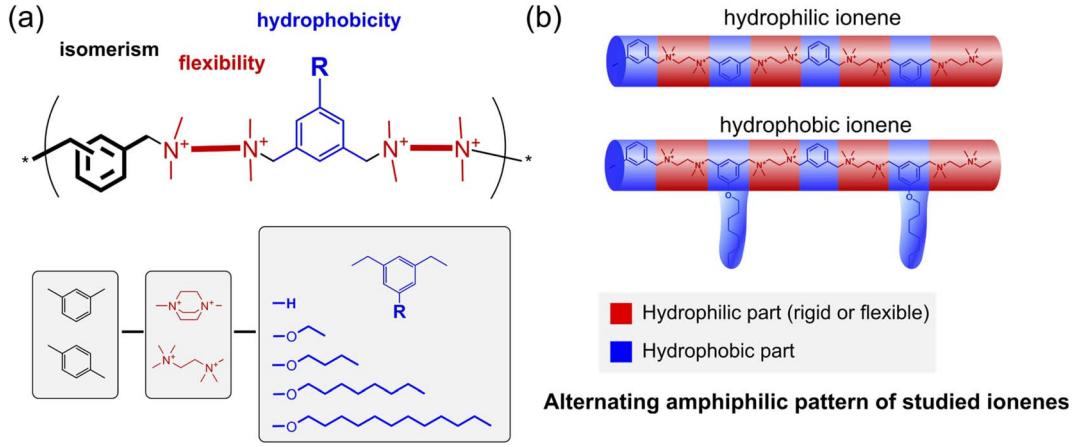

Fig. 1 (a) The concept of the ionenes library, which allows for investigating the cross-influence between the isomerism, flexibility, and hydrophobicity on the antimicrobial activity; (b) a schematic illustration of the alternating amphiphilicity pattern of the studied ionenes based on recent work by Z. Chen *et al.*[38]

the molecule to incorporate into the membrane interior.[14,16] Therefore, the elevated conformational freedom seems to facilitate such conformational changes and in turn influence antimicrobial potency.[15] However, there is a scarcity of systematic studies reported on the impact of the polycationic main-chain flexibility on their activity. This problem has been broadly investigated in the case of AMPs, but in most of these studies, the flexibility modulation involved additional changes in the overall hydrophobicity.[17–20] It may be expected that different conformers interact with a membrane with different strengths; therefore, polycationic mainchain topology, which determines the possible conformations, may also potentially affect the antimicrobial activity. It has been reported that the topology of ionenes (polycations with cationic groups inside the main-chain), in terms of an aryl group isomerism, strongly impacts their behavior in water solution,[21–23] which supports the above hypothesis. Hydrophilic-lipophilic balance (HLB) is another important and well-studied structural parameter that strongly influences the conformational changes and penetration of the phospholipid bilayer. A large body of experimental data indicates that it is hard to establish a general rule describing the optimal level of HLB for high antimicrobial activity and selectivity. Each polycationic system requires an individual fine-tuning of this parameter.[24–30] Among the studied polycationic architectures, we identified a class of relatively hydrophilic ionenes as especially interesting due to their excellent selectivity toward microbes over red blood cells (RBCs).[31–38]

Mycobacteria contain a complex and strongly hydrophobic cell wall consisting of the peptidoglycan-arabinogalactan-mycolic acid complex, with mycolic acids located at the outer layer.[39,40] H. Chen *et al.*, in their review, have pointed to the mycobacterial membrane as a novel target for anti-tuberculosis drugs, such as cationic amphiphiles.[39] Low-molecular-weight cationic amphiphiles,[41] cationic dendrimers,[42] AMPs,[43,44] cationic polymers,[33,45–48] and gold nanoparticles coated with polycations,[49] highly active against mycobacteria, have been reported to date. Most of those studies were performed on *Mtb* and *Mycobacterium smegmatis* (*Mms*), which is frequently employed as an avirulent and fast-growing model organism for *Mtb*, especially in mechanistic studies.[50,51] Besides inhibitory growth activity, the abovementioned polycations display high mycobactericidal efficiency against *Mtb* and *Msm* at concentrations close to the minimum inhibitory concentration (MIC).[41,45–47] Reported data have indicated a disruption of the mycobacterial membrane or morphological changes in a cell envelope under the influence of polycations.[45–47] However, a possible intercellular mode of action was discussed.[52] Intriguingly, the high selectivity toward mycobacteria over *Staphylococcus aureus* and *Escherichia coli* has been observed for some polycations.[42,46–49] This reflects differences in the cell envelope structures of these bacteria, and highlights a possibility that cationic amphiphiles not active against Gram-negative and Gram-positive species may be highly active against *Mtb*.

In this work, we investigate the cross-influence of hydrophobicity, main-chain flexibility, and isomerism of ionenes on their antimicrobial activity against model microorganisms and drug-resistant clinical isolates, including mycobacteria. Besides the antimicrobial activity, the critical aggregation concentrations (CAC) and zeta-potential of the aggregates were also determined. To fulfill this task, a broad library of ionenes (Fig. 1a) characterized by an alternating amphiphilic pattern (Fig. 1b) was developed. The library consisted of already published structures and newly synthesized ones to summarize a broader investigation effort.

2. Experimental section

2.1 Materials

All chemical reagents were purchased from Sigma-Aldrich, TCI Chemicals, Fluorochem, or Chempur, and were used without further purification. Regenerated-cellulose dialysis tubing (Spectra/Por® 7, MWCO 1 kDa) was pre-treated according to the instruction provided by the manufacturer. Water for dialysis,

antimicrobial assays, and SEC analysis was purified with a Milli-Q system (Millipore). Freeze-drying was performed using Labconco FreeZone ® 2.5 Liter Benchtop Freeze Dry Systems. Broths for antimicrobial assays were prepared using commercially available Mueller–Hinton Broth powder (Biocorp) and Sabouraud broth (SAB) powder containing 2% dextrose (Merck). As a solid medium for colony plate counting, commercially available Mueller–Hinton 2 containing agar (Biocorp) and Sabouraud containing agar (BioMaxima) powders were used. Buffered phosphate saline solution pH 7.4 (PBS) was prepared from 10× solution (Fisher BioReagents™) by dilution with Milli-Q water. American Type Culture Collection (ATCC) bacterial and yeast strains were used in this work: *Escherichia coli* (ATCC 8739), *Staphylococcus aureus* (ATCC 6538), *Candida albicans* (ATCC 10231), *M. tuberculosis* H37Rv strain (ATCC 25618), *M. avium* (ATCC 15769), and *M. terrae* (ATCC 15755). Clinical isolates: *M. tuberculosis* Spec. 210 (isoniazid resistant, INH-R), *M. tuberculosis* Spec. 192, *K. pneumoniae* (metallo-β-lactamase MBL), *K. pneumoniae* (extended-spectrum β-lactamase ESBL), *E. faecium* (vancomycin resistant, VRE), *P. aeruginosa*, *S. aureus* (methyciline resistant, MRSA), and *A. baumanii* were obtained from the collection of pathogenic strains of the Microbiology Department of the National Tuberculosis and Lung Diseases Research Institute (Warsaw, Poland). All of those strains were isolated from patients hospitalized at the National Tuberculosis and Lung Diseases Research Institute between 2019 and 2021, and kept frozen at −80 °C prior to use.

2.2 Characterization of chemical compounds

The ^{1}H and ^{13}C NMR spectra were recorded using a Varian 400 MHz spectrometer and D_2O or $CDCl_3$ as solvents. ^{1}H NMR chemical shifts were referenced to the residual signal of the protonated solvent (δ 7.26 for $CDCl_3$ and 4.79 for D_2O). ^{13}C NMR chemical shifts were referenced to the solvent (δ 77.16 for $CDCl_3$). Elemental analyses were performed using a Vario EL III CHNS Elemental instrument.

SEC analysis was performed using an Agilent 1260 Infinity liquid chromatograph equipped with RID and UV DAD detector (detection at 268 nm), the PSS NOVEMA Max 5 μm analytical 300 × 8 mm column with precolumn (PSS GmbH), a mobile phase containing: 54/23/23 (v/v/v%) water/methanol/acetic acid and 0.5 M sodium acetate. All used chemicals were HPLC grade. To calibrate the SEC method, a series of poly(2-vinylpyridine) standards (PSS GmbH) in the range of molar masses of 620 Da–539 kDa were used. Samples, dissolved in the eluent at 5 mg mL^{-1} concentrations, were injected in 20 μL volumes. Analysis was performed at 50 °C at a flow rate of 0.4 mL min^{-1}. The molar masses M_w, M_n, and dispersities $Đ_M$ were calculated using the Agilent GPC Addon Rev. B.01.02 software. The dynamic light scattering measurements were performed using a Zetasizer Nano from Malvern Instruments UK. Particle size (by scattering intensity) and zeta-potential were calculated using the software provided by Malvern. Dynamic light scattering was measured at a scattering angle of 173°. Zeta-potential was calculated from measured electrophoretic mobility by applying Smoluchowski's equation.

2.3 Material synthesis

Ionenes C0-T-p,[53] C8-T-p,[53] C0-T-m,[31] 1-alcoxy-3,5-bis(bromomethyl)benzenes (**1-C*n***)53 and α,α′-bis(1-azonia-4-azabicyclo[2.2.2]octyl)-para-xylene dibromide (**2**)[31] were obtained as reported previously.

α,α′-Bis(*N*,*N*,*N*′,*N*′-tetramethyl-ethylene-1-ammonium-2-amine)-meta-xylene dibromide (**3**). A solution of α,α′-dibromo-*m*-xylene (4.75 g, 18 mmol) in MeCN (120 mL) was added dropwise at room temperature to a stirred solution of TMEDA (16.3 mL, 12.5 g, 108 mmol) in MeCN (72 mL) over 30 min, and the reaction mixture was refluxed overnight. After cooling down to room temperature, the homogenous mixture was concentrated on a rotatory evaporator. The obtained oil was dissolved in MeCN (30 mL) and poured into diethyl ether (300 mL), facilitating precipitation of a sticky solid. The solid was washed using MeCN (40 mL) and cooled to −40 °C MeCN (100 mL). The obtained crystalline solid was then dried under vacuum overnight, yielding a strongly hygroscopic white solid (8.93 g, 77%). ^{1}H NMR (400 MHz, D_2O) δ: 2.25 (12H, s), 2.91 (4H, m), 3.06 (12H, s), 3.48 (4H, m), 4.59 (4H, s), 7.71 (4H, m); ^{13}C NMR (400 MHz, D_2O) δ: 137.29, 135.44, 130.37, 128.12, 67.93, 61.33, 50.83, 50.00, 44.40.

2.3.1 C*n*-D-p ionenes. The following represents a general procedure for the synthesis of all C*n*-D-p ionenes.

C2-D-p. A solution of 1-ethoxy-3,5-bis(bromomethyl)benzene (**1-C2**) (1.109 g, 3.60 mmol) in DMSO (4 mL) was added dropwise, at room temperature, to a stirred solution of α,α'-(1-azonia-4-azabicyclo[2.2.2]octyl)-*p*-xylene dibromide (**2**) (1.932 g, 3.96 mmol), DMSO (26 mL) and water (2 mL). The reaction mixture was stirred at room temperature for 24 h and poured into acetone (400 mL). The obtained suspension was centrifuged, and the supernatant was removed. Subsequently, the solid was preliminarily dried, dissolved in water (160 mL), transferred to dialysis tubing (MWC 1 kDa), and dialyzed against Milli-Q water for 3 days. The solution was freeze-dried, yielding 1.495 g (49%) of white powder. Found: C, 40.37; H, 6.36; N, 6.57%; $(C_{30}H_{44}Br_4N_4O\cdot 5H_2O)_n$ requires: C, 40.65; H, 6.14; N, 6.32%. ^{1}H NMR (400 MHz, D_2O) (integrals for repeating units) δ: 1.33 (t, 3H), 3.12 (m, 6H, terminal), 3.44 (m, 6H, terminal), 4.03 (m, 26H), 4.53 (s, 4H, terminal group), 4.84 (m, 8H), 7.28 (s, 3H), 7.70 (m, 4H).

C4-D-p (20%). Found: C, 42.06; H, 6.78; N, 6.39%; $(C_{32}H_{48}Br_4N_4O\cdot 5H_2O)_n$ requires: C, 42.03; H, 6.39; N, 6.13%. ^{1}H NMR (400 MHz, D_2O) (integrals for repeating unit) δ: 0.87 (t, 3H), 1.40 (m, 2H), 1.70 (m, 2H), 3.11 (m, 6H, terminal group), 3.44 (m, 6H, terminal group), 4.02 (m, 26H), 4.52 (s, 4H, terminal group), 4.84 (m, 8H), 7.28 (s, 3H), 7.70 (m, 4H).

C8-D-p (60%). Found: C, 44.03; H, 7.09; N, 5.86%; $(C_{36}H_{56}Br_4N_4O\cdot 6H_2O)_n$ requires: C, 44.55; H, 6.85; N, 5.77%. ^{1}H NMR (400 MHz, D_2O) (integrals for repeating unit) δ: 0.89–1.74 (m, 15H), 3.13 (m, 6H, terminal), 3.43 (m, 6H, terminal), 4.03 (bs, 26H), 4.79 (s, 4H, terminal group), 4.79 (s, 8H), 7.29 (s, 3H), 7.76 (m, 4H).

C12-D-p (53%). Found: C, 48.85; H, 7.82; N, 5.82%; $(C_{32}H_{48}Br_4N_4O\cdot 6H_2O)_n$ requires: C, 48.50; H, 7.12; N, 5.66%. ^{1}H NMR (400 MHz, DMSO-d_6) (integrals for repeating unit) δ: 0.83

(m, 3H), 1.22–1.37 (m, 18H), 1.70 (bs, 2H), 3.00 (m, 6H, terminal), 3.36 (m, 6H, terminal), 4.00 (m, 26H), 4.92 (s, 4H, terminal group), 4.87 (bs, 8H), 7.01–7.37 (m, 3H), 7.65–7.72 (m, 4H).

C0-D-p (30%). Found: C, 38.13; H, 6.17; N, 6.42%; $(C_{36}H_{64}Br_4N_4O\cdot 7H_2O)_n$ requires: C, 38.29; H, 6.20; N, 6.38%. ^{1}H NMR (400 MHz, D_2O) (integrals for repeating unit) δ: 3.12 (m, 6H, terminal group), 3.44 (m, 6H, terminal group), 4.02 (m, 26H), 4.53 (s, 4H, terminal group), 4.84 (m, 8H), 7.28 (s, 3H), 7.64–7.73 (m, 8H).

2.3.2 C*n*-T-m ionenes. The following represents a general procedure for the synthesis of all C*n*-T-m ionenes.

C2-T-m. A solution of 1-ethyloxy-3,5-bis(bromomethyl) benzene (**1-C2**) (1.109 g, 3.60 mmol) in DMSO (4 mL) was added dropwise, at room temperature, to a stirred solution of **3** (1.964 g, 3.96 mmol), DMSO (5.6 mL) and water (2 mL). The reaction mixture was stirred at room temperature for 24 h and poured into acetone (400 mL). The obtained suspension was centrifuged, and the supernatant was removed. Subsequently, the solid was dried, dissolved in water (160 mL) and transferred to dialysis tubing (MWC 1 kDa) and dialyzed against Milli-Q water for 3 days. The solution was freeze-dried, yielding 1.495 g (49%) of white powder. Found: C, 41.54; H, 7.03; N, 6.55%; $(C_{30}H_{52}Br_4N_4O\cdot 4H_2O)_n$ requires: C, 41.11; H, 6.90; N, 6.39%. ^{1}H NMR (400 MHz, D_2O) (integrals for repeating unit) δ: 1.34 (t, 3H), 2.33 (s, 6H, terminal group), 2.91 (m, 2H, terminal group), 3.07 (s, 6H, terminal group), 3.20 (bs, 24H), 3.45 (m, 2H, terminal group), 4.14–4.21 (m, 10H), 7.35–7.46 (m, 3H), 7.67–7.77 (m, 4H).

C4-T-m (34%). Found: C, 41.89; H, 7.18; N, 6.33%; $(C_{32}H_{56}Br_4N_4O\cdot 4H_2O)_n$ requires: C, 42.49; H, 7.13; N, 6.19%. ^{1}H NMR (400 MHz, D_2O) (integrals for repeating unit) δ: 0.83 (t, 3H), 1.36 (m, 2H), 1.68 (m, 2H), 2.22 (s, 6H, terminal group), 2.90 (m, 2H, terminal group), 3.06 (s, 6H, terminal group), 3.20 (bs, 24H), 3.44 (m, 2H, terminal group), 4.08–4.20 (m, 10H), 7.35–7.45 (m, 3H), 7.68–7.76 (m, 4H).

C8-T-m (34%). Found: C, 43.79; H, 7.51; N, 5.84%; $(C_{36}H_{64}Br_4N_4O\cdot 6H_2O)_n$ required: C, 43.38; H, 7.69; N, 5.62%. ^{1}H NMR (400 MHz, D_2O) (integrals for repeating unit) δ: 0.74 (t, 3H), 1.14–1.33 (m, 12H), 1.65 (m, 2H), 2.32 (s, 6H, terminal group), 3.06 (m, 2H, terminal group), 3.06 (s, 6H, terminal group), 3.20 (bs, 24H), 3.50 (m, 2H, terminal group), 4.09–4.20 (m, 10H), 7.37–7.44 (m, 3H), 7.68–7.76 (m, 4H).

C12-T-m (68%). Found: C, 46.15; H, 7.69; N, 5.09%; $(C_{40}H_{72}Br_4N_4O\cdot 5H_2O)_n$ required: C, 46.43; H, 7.99; N, 5.41%. ^{1}H NMR (400 MHz, CD_3OD) (integrals for repeating unit) δ: 0.90 (t, 3H), 1.29–1.48 (m, 12H), 1.78 (m, 2H), 2.33 (s, 6H, terminal group), 2.88 (m, 2H, terminal group), 3.20 (s, 6H, terminal group), 3.41 (m, 24H), 3.58 (m, 2H, terminal group), 4.08 (bs, 2H), 4.42 (bs, 8H), 7.09–7.91 (m, 7H).

2.4 Minimum inhibitory concentration (MIC) determination for model strains

The broth microdilution method was applied following CLSI M07-A9 vol. 32 no. 2 (for bacteria) and CLSI M27-A2 vol. 22 no. 15 (for yeast) protocols. Single colonies of bacteria or yeast were used to inoculate 5 mL of Mueller–Hinton Broth (MHB) or Sabouraud broth, respectively, and the cultures were grown overnight at 37 °C with shaking (240 rpm; Lab Companion SI-600R, Ramsey, MN, USA). The polymer stock solutions of 5120 μg mL^{-1} prepared in Milli-Q water were diluted with a broth (MHB or SAB) to a concentration of 1024 μg mL^{-1}, and used to prepare a series of different polymer concentrations (from 512 μg mL^{-1} to 2 μg mL^{-1}; 100 μL each) in 96-well plates by two-fold dilution method. Subsequently, 100 μL of microbial suspension (2×10^5 CFU mL^{-1} for bacteria and 2×10^3 CFU mL^{-1} for yeast) was added to each well. Uninoculated broth, uninoculated broth with polymer solutions, and inoculated broth without any antimicrobial agent were used as controls. Four replicates were performed for each concentration of polymer and the control. The plates were incubated for 20 h at 37 °C. The optical density at 600 nm (OD_{600}) was measured using a Synergy™ H4 Hybrid Microplate Reader, Biotech (Winooski, VT, USA). The recorded MIC value was the lowest concentration of the polymer at which no microbial growth was observed with the microplate reader.

2.5 MIC against *Mycobacterium*

The assay was performed by the two-fold serial microdilution method (in 96-well microliter plates) using Middlebrook 7H9 Broth medium (Beckton Dickinson) containing 10% of OADC (Beckton Dickinson). The inoculum was prepared from fresh LJ culture in Middlebrook 7H9 Broth medium with OADC, adjusted to a no. 0.5 McFarland tube, and diluted to 1 : 20. The stock solution of a tested molecule was prepared in water and diluted in Middlebrook 7H9 Broth medium with OADC by four-fold the final highest concentration to be tested. Compounds were diluted serially in sterile 96-well microtiter plates using 100 μl Middlebrook 7H9 Broth medium with OADC. Concentrations of the tested agents ranged from 0.25 to 512 μg mL^{-1}. A growth control containing no antibiotic and a sterile control without inoculation were also prepared on each plate. After incubation, (*Mycobacterium avium* for 7 days, and *Mycobacterium terrae*, *Mycobacterium tuberculosis* strains at 37 °C for 21 days), the MICs were visually assessed as the lowest concentration showing complete growth inhibition of the reference microbial strains. Isoniazid (INH) and Rifampicin (RMP) were used as the reference drugs.

2.6 MIC against clinical isolates

The assay was performed by the two-fold serial microdilution method (in 96-well microliter plates) using MHB medium (Sigma). The inoculum was prepared from fresh Columbia agar (BioMerieux) culture in MHB medium, adjusted to a no. 0.5 McFarland tube, and diluted to 1 : 20. The stock solution of a tested molecule was prepared in water and diluted in MHB medium by four-fold the final highest concentration to be tested. Compounds were diluted serially in sterile 96-well microtiter plates using 100 μl MHB medium with OADC. Concentrations of the tested agents ranged from 0.25 to 512 μg mL^{-1}. A growth control containing no antibiotic and a sterile control without inoculation were also prepared on each plate. After incubation (bacterial strains at 35 °C for 24 h), the MICs

were visually assessed as the lowest concentration showing complete growth inhibition of the reference microbial strains. Ciprofloxacin was used as the reference drug.

2.7 Time-kill kinetics assay

A single colony of *S. aureus* was used to inoculate 5 mL of MHB, and the culture was grown overnight at 37 °C with shaking (240 rpm). Then, after a 1 : 100 dilution in fresh growth media, the cultures were further incubated at 37 °C with shaking until $OD_{600} = 0.6$ and diluted by 1 : 100 in fresh media again to *ca.* 10^5 CFU mL^{-1}. The bacteria suspension (180 μL) was added to the water polymer solution (20 μL) at a concentration of 10, 20, and 40 × MIC, which resulted in the final polymer concentration of 1, 2, and 4 × MIC, respectively. The suspensions were incubated at 37 °C, 20 μL samples were collected after 5, 10, 20, 40, 60 min, and a series of tenfold dilutions using phosphate buffer solution were prepared. Growth medium-treated cultures served as a positive control of bacterial growth. The final dilutions (10 μL) were spread on agar plates with MHA, and left for incubation for 20 h at 37 °C. After incubation, the colony-forming units were counted.

2.8 Hemolytic activity determination

Fresh blood was obtained from the Regional Center for Blood Donation and Blood Treatment in Warsaw. Samples were centrifuged (700*g*, 10 min), the supernatant plasma was rejected, and erythrocytes were washed with ice-cold phosphate-buffered saline (PBS) three times (by centrifuging, 700*g*, 10 min). After the final centrifugation, erythrocytes were diluted ten times with PBS. Polymer solutions were prepared in PBS buffer. Erythrocyte suspensions (500 μL) were added to polymer solutions (500 μL) at the investigated concentrations. Samples were incubated for 1 h at 37 °C, and then the samples were centrifuged (10 min, 700*g*). The hemoglobin release was subsequently measured in the supernatants using the spectrophotometric method (absorption at $\lambda = 540$ nm). PBS buffer and 0.2% Triton X-100 served as the negative and positive controls, respectively. Experiments were performed at the Faculty of Chemical and Process Engineering WUT with the local committee approval for research with human blood.

3. Results and discussion

3.1 Polymer design, synthesis, and characterization

To investigate the cross-influence of the hydrophobicity, main-chain flexibility, and topology of ionenes on their antimicrobial and hemolytic activity, a library of ionenes composed of newly synthesized molecules and already reported structures[31,53,54] was used (Fig. 1a). The molecules characterized by different topologies contain *meta* or *para* isomers of an aromatic linker, whereas the molecules characterized by different flexibilities contain 1,4-diazabicyclo[2.2.2]octane (DABCO) or tetramethylethylenediamine (TMEDA) subunit along the main-chain. The hydrophobicity was modulated by the length of the side alkyl group.

Ionenes from the series C*n*-D-m and C*n*-T-p, and ionene C0-T-m, were obtained and characterized in previously published works.[31,53,54] The synthesis and characterization of the flexible *meta*-ionenes (C*n*-T-m) and rigid *para*-ionenes (C*n*-D-p) are presented herein for the first time. To obtain the desired polycations monomers, **1-C*n***, **2**, and **3** were synthesized according to Schemes 1 and S1.† Dibromides **1-C*n*** were obtained by *O*-alkylation of 5-hydroxyisophthalate, and a subsequent ester reduction with lithium aluminum hydride (LAH) followed by bromination with PBr_3 (Scheme S1†).[53] Tertiary amines **2** and **3** were obtained by treating the *para* (1,4-) and *meta* (1,3-) isomers of bis(bromomethyl)benzene with an excess of DABCO[31] and TMEDA, respectively. A polyaddition reaction between dibromides **1-C*n*** and diamines **2** and **3**, using 10% molar excess, led

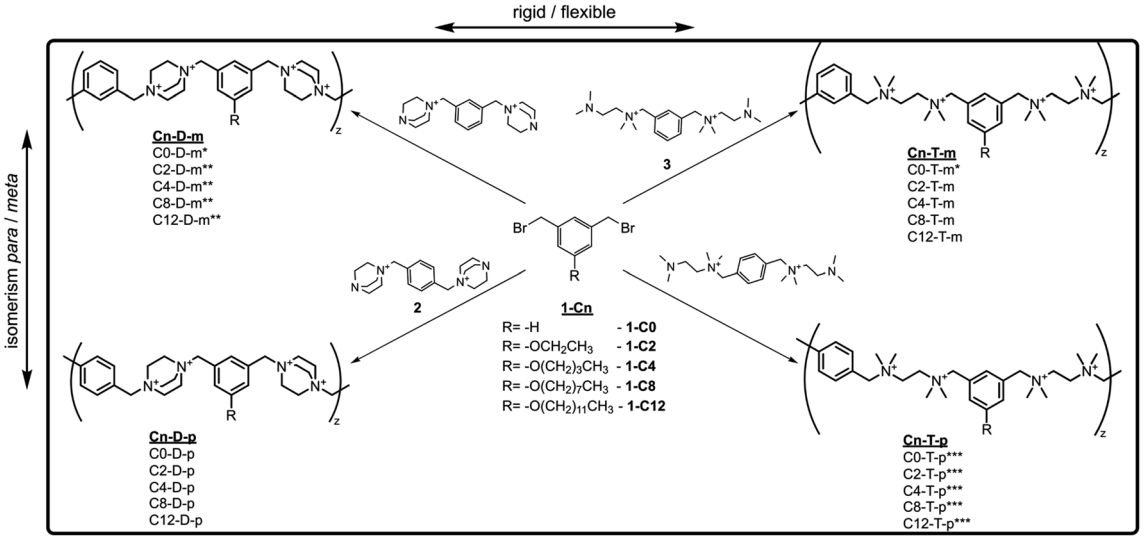

Scheme 1 The synthetic pathway of the investigated ionenes; the polyaddition reactions were conducted in a DMSO/water mixture at room temperature using 10% molar excess of di-amines. * from ref. 31, ** from ref. 54, *** form ref. 53.

to the final polycations. This approach enabled the obtaining of different ionenes characterized by a similar average molecular mass and well-defined terminal groups.[31,55]

The polymer structures were confirmed *via* ^{1}H NMR spectroscopy. Owing to the known chemical shifts of the polymer terminal groups,[31] the degree of polymerization (DP) and the number average molar mass ($M_{n,\ NMR}$) were calculated (Fig. 2 and Table 1). The DP falls within the range of 7.3–13.8. The ionenes were further characterized by size exclusion chromatography (SEC), which confirmed a similar molecular mass distribution (Fig. 2b). The number of the average molecular mass determined by SEC ($M_{n,SEC}$) remained in the range of 4.0–7.5 kDa for ionenes containing the pendant alkyl chain up to 8 carbon atoms, and the obtained values correlate well with $M_{n,NMR}$. For ionenes with the dodecyloxy pendant group, the $M_{n,SEC}$ falls in the range of 2.3–3.3 kDa, and it is significantly lower than the $M_{n,NMR}$, which likely is a result of the hydrophobic interaction between the tested molecules and the stationary phase of the chromatographic column. Polymer dispersity ($Đ$) remains in the range between 1.38 to 1.85.

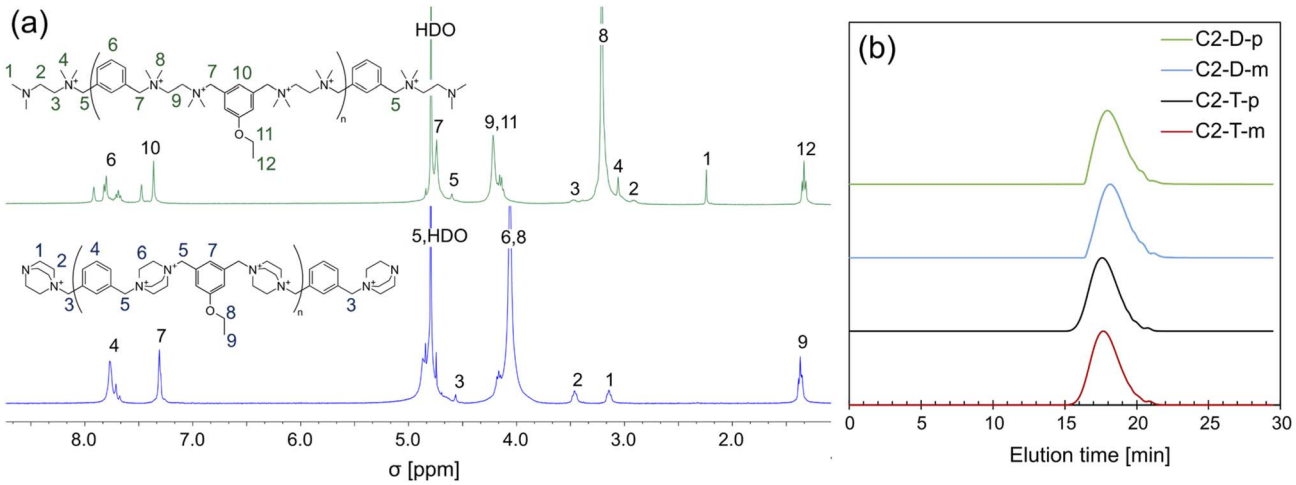

Fig. 2 (a) Example of the ^{1}H NMR spectra of the rigid and flexible ionenes, and (b) SEC traces of ionenes containing the ethylene pendant group. For full characterization of all ionenes, see ESI.†

Table 1 Characterization of obtained ionenes

Polymer	DP[a]	$M_{n,NMR}$[b] [kDa]	$M_{n,SEC}$[c] [kDa]	$Đ$[c]	CAC[d] [μg mL^{-1}]		Zeta potential[e] [mV]	
					H_2O	PBS	H_2O	PBS
C0-D-*m**	10.6	4.6	4.8	1.73	>2000	>2000	n.d[f]	n.d.[f]
C2-D-*m***	11.8	5.6	4.6	1.77	>2000	>2000	n.d[f]	n.d.[f]
C4-D-*m***	10.4	5.2	5.3	1.63	>2000	>2000	n.d[f]	n.d.[f]
C8-D-*m***	9.0	5.0	4.5	1.73	360	38	65.0 ± 1.4	14.1 ± 1.6
C12-D-*m***	11.9	7.3	2.3	1.43	20	≤4	67.0 ± 2.7	19.5 ± 2.1
C0-D-*p*	10.1	4.4	4.4	1.85	>2000	>2000	n.d[f]	n.d[f]
C2-D-*p*	11.6	5.5	5.2	1.79	>2000	>2000	n.d[f]	n.d[f]
C4-D-*p*	9.1	4.6	4.0	1.67	>2000	>2000	n.d[f]	n.d[f]
C8-D-*p*	11.0	6.2	4.1	1.80	1100	49	46.6 ± 1.3	17.3 ± 0.2
C12-D-*p*	9.2	5.7	2.3	1.38	53	15	60.4 ± 1.0	17.3 ± 1.1
C0-T-*m**	7.3	3.2	4.0	1.48	>2000	>2000	n.d.[f]	n.d.[f]
C2-T-*m*	12.8	6.2	6.9	1.80	>2000	>2000	n.d.[f]	n.d.[f]
C4-T-*m*	13.0	6.7	6.7	1.82	>2000	>2000	n.d.[f]	n.d.[f]
C8-T-*m*	12.4	7.1	5.5	1.82	1600	600	82.1 ± 3.1	23.6 ± 1.6
C12-T-*m*	12.7	7.9	4.9	1.34	56	10	97.2 ± 1.7	31.3 ± 2.0
C0-T-*p****	12.2	5.4	7.3	1.78	>2000	>2000	n.d[f]	n.d[f]
C2-T-*p****	12.4	6.0	7.5	1.79	>2000	>2000	n.d.[f]	n.d.[f]
C4-T-*p****	10.9	5.6	6.7	1.84	>2000	>2000	n.d.[f]	n.d.[f]
C8-T-*p****	13.8	7.9	6.5	1.82	>2000	920	n.d.[f]	18.2 ± 0.9
C12-T-*p****	10.6	6.6	3.3	1.46	80	16	64.1 ± 0.6	16.9 ± 1.5

[a] DP determined from ^{1}H NMR spectra. [b] $M_{n,NMR}$ calculated using DP and the molar mass of a repeating unit without bromides. [c] $M_{n,SEC}$ and $Đ$M determined by size exclusion chromatography (SEC). [d] the critical aggregation concentration (CAC) was determined by pyrene method. [e] zeta potential of polymeric aggregates determined by DLS technique at a concentration of 2 mg mL^{-1}. [f] Not determined. * from ref. 31. ** from ref. 54. *** from ref. 53.

The critical aggregation concentration (CAC) of the polymers in pure water and phosphate-buffered saline pH 7.4 (PBS) was determined using the pyrene method.[56] Ionenes without an alkyl group (C0) and with C2 and C4 groups do not form aggregates at a concentration of up to 2000 μg mL^{-1} (Table 1), whereas C8 derivatives show CAC within a range of 38–1600 μg mL^{-1} and C12 derivatives within a range of less than 4 μg mL^{-1} to 110 μg mL^{-1}. Besides an obvious relationship between the hydrophobicity and CAC, a systematic influence of the flexibility and isomerism can be perceived. More rigid DABCO-containing ionenes showed lower CAC values than their flexible counterparts. Comparing the ionenes containing *meta-* or *para*-substituted aryl linkers, lower CAC values may be observed for the former ones. This indicates that the increased stiffness of the polymeric main-chain and incorporation of *meta* isomers of the aryl moiety enhance the formation of aggregates. Polymeric aggregates were studied employing the dynamic light scattering technique (DLS) to determine their hydrodynamic size and zeta-potential. Size distributions for all studied polycations at a concentration above the CAC were multimodal. Therefore, they are not discussed herein. Zeta-potential measurements indicated a relatively high positive electrokinetic charge on the surface of the aggregates, which is higher for the more flexible TMEDA-containing ionenes and for the *meta* isomers in comparison to the *para* ones.

3.2 Antimicrobial and hemolytic activity

3.2.1 Activity against model microorganisms. Determination of the minimum inhibitory concentration (MIC) against the model, clinically relevant microorganisms (*Escherichia coli*, *Staphylococcus aureus*, and *Candida albicans*) from the American Type Culture Collection (ATCC), allowed for the comparison of the antimicrobial activity of all discussed ionenes. Data collected for the C*n*-D-p and C*n*-T-m polymers are presented in Fig. 3 along with the previously reported[31,53,54] MIC values for C*n*-D-m and C*n*-T-p polymers. Results display a wide range of activity levels among the studied ionenes, from highly potent (MIC 2–8 μg mL^{-1}) to relatively weak (MIC 128–256 μg mL^{-1}). Gram-positive *S. aureus* was more susceptible toward the polycations than Gram-negative *E. coli*, whereas the fungi *C. albicans* was the most resistant among the tested microorganisms. Such observations were also reported for other cationic polymers.[34,36,48,57–60] Gram-negative bacteria, in contrast to Gram-positive ones, are characterized by a presence of the outer cell membrane, which hinders polycations from reaching the inner membrane. Furthermore, fungi *C. albicans* is a eukaryotic organism covered with a complex cell wall, and a cell membrane characterized by a lower amount of anionic phospholipids in comparison to the bacterial membrane.[61,62] Differences in the cell envelope structures were proposed to explain the variation in the activity of the polycations.[14]

To facilitate further discussion, this section is divided into two short parts – in the first part, the influence of

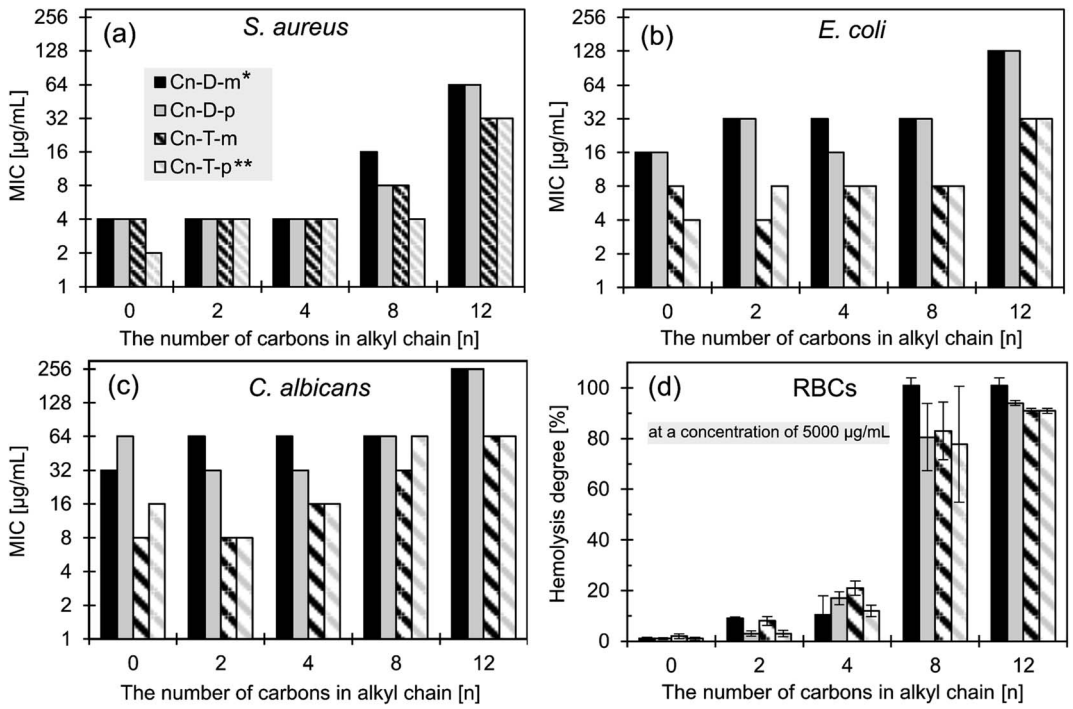

Fig. 3 Antimicrobial activity of the studied ionenes toward model microorganisms: (a) *S. aureus* (ATTC 6538), (b) *E. coli* (ATTC 8739), and (c) *C. albicans* (ATCC 10231); (d) the degree of hemolysis (human RBCs) induced by the fixed polymers concentration (5000 μg mL^{-1} for $n = 0$, 2, 4, 8, and 2.5 mg mL^{-1} for $n = 12$). Data for polymers C0-D-m and C0-T-m from the ref. 31; * from the ref. 54, ** from the ref. 53.

hydrophobicity and isomerism is discussed, whereas the second part covers the flexibility effect on the growth inhibitory activity.

3.2.2 Hydrophilic–lipophilic balance and main-chain isomerism. Within each polycationic series, the most hydrophobic derivatives, bearing the C12 alkyl group, display the highest MICs (32–256 μg mL^{-1}) against all microorganisms (Fig. 3a–c). On the other hand, MICs of ionenes without pendant groups (C0-T-p, C0-T-m, C0-D-p, C0-D-m) are the lowest or comparable with ionenes containing short alkyl chains (2–64 μg mL^{-1}). The impact of HLB is clearly dependent on the microorganism. In the case of *E. coli*, ionenes with alkyl groups up to C8 show rather comparable MICs within each series. However, C0 ionenes seem to be the most active (Fig. 3b). Ionenes C0, C2, and C4 are equally active against *S. aureus*, and the impact of the increased hydrophobicity is clearly visible for the C8 and C12 ionenes (Fig. 3b). Considering the activity against *C. albicans*, a similar activity of DABCO containing C0, C2, C4, and C8 ionenes may be noticed, whereas MICs of the TMEDA-containing derivatives show a tendency to increase from C0 and C2 to the C8 ionenes. The shown data confirm that the increased hydrophobicity of the pendant group in the discussed series of polymers reduces the antimicrobial activity. An explanation of this phenomena was proposed in our recently published work.[53]

It has been widely reported that the HLB of amphiphilic polycations must be fine-tuned to obtain the most potent antimicrobial macromolecules, and the optimal position is strongly dependent on the polycationic mainchain structure.[15,63] For example, the Tew group reported the optimum HLB for polynorbornenes when propyl and butyl alkyl moieties were incorporated.[64] Polycarbonates reported by the Hedrick and Yang groups were the most active with a hexyl moiety,[26] whereas polyvinylpyridine derivatives reported by the Sen group displayed the lowest MIC with a butyl or hexyl group.[24] In light of the published data, we can conclude that the optimal HLB value of the discussed ionenes herein is rather shifted toward hydrophilic structures.

The isomerism of aryl linkers displays a negligible influence on the antimicrobial activity, and no correlation is visible. The isomerism determines the possible conformations that the ionene molecules may attain. It hypothetically can modulate the interactions with a cell membrane and wall. The isomerism effect was observed for relatively hydrophilic ionenes without pendant groups in our previous work,[31] and by Mayr *et al.*[65] However, the results presented herein indicate that the effect is negligible for the ionenes containing higher hydrophobic side groups.

3.2.3 Flexibility of the main-chain. In the majority of cases, ionenes with a flexible TEMDA linker display higher antimicrobial activity in comparison to their DABCO-containing counterparts. However, the effect depends strongly on the antimicrobial strain and ionenes hydrophobicity. The flexible ionenes are more active against Gram-negative *E. coli* and fungi *C. albicans* over almost the entire range of alkyl chain lengths. In contrast, against Gram-positive *S. aureus*, the flexibility effect is only visible for the more hydrophobic molecules (C8 and C12 series). The discrepancies are likely related to differences in the cell envelope structure, through which the polycationic molecules diffuse, and the cell membrane composition, being considered as the most important target for these molecules.

The elevated activity of the more flexible polymers could be explained by the hypothesis concerning the important role of the conformational freedom in the modulation of interactions between the polycations and the cell membrane.[15] The flexible structure allows a molecule to attain a higher number of conformations separated with lower energy barriers. It may facilitate both a migration through a bacterial cell envelope and a formation of the most energetically privileged assembly between a polycation and a lipid bilayer upon binding to a water–lipid interface. However, when compared with the flexible ionenes (Table 1), the lower CAC values of the rigid ionenes, which point to their higher tendency to aggregation, and the lower zeta-potential of those aggregates may also be responsible for their lower activity.

3.2.4 Hemolytic activity. Hydrophobicity is the only structural parameter significantly influencing hemolytic activity within the library of investigated polycations. The most hydrophilic ionenes without pendant groups are non-hemolytic at 5 mg mL^{-1} (Fig. 3d). Slightly more hydrophobic polycations with ethyl and butyl pendant groups are mild hemolytic agents, whereas strongly hydrophobic polycations with octyl and dodecyl groups reached 80–100% degree of hemolysis at the studied concentrations. The concentration of the ionenes causing hemolysis of 50% of RBCs in the sample (HC_{50}) for the C0-, C2- and C4-ionenes exceeds 5000 μg mL^{-1}. The comparison between the very low MICs value of C0-ionenes and HC_{50} (higher than 5000 μg mL^{-1}) results in a selectivity index greater than 1250. Intriguingly, hydrophobicity has an opposite impact on the antimicrobial and hemolytic activity of ionenes. Similar observations were reported by S. N. Riduan *et al.* for imidazolium-based ionenes containing alkyl terminal groups.[66] This effect is likely derived from the different cell envelope structure and lipid composition between the bacterial and RBC's membranes.

3.2.5 Activity against clinical strains including m*Mycobacterium*. The influence of the main-chain flexibility and overall hydrophobicity on the antibacterial activity of ionenes was further explored using clinically isolated bacteria, including antibiotic-resistant strains and *Mycobacterium* species. In those studies, the following microorganisms were used: two strains of *Klebsiella pneumoniae* producing New Delhi metallo-β-lactamases (MBL, NDM type) and extended-spectrum β-lactamases (ESBL), vancomycin-resistant *Enterococcus faecium* (VRE), methicillin-resistant *Staphylococcus aureus* (MRSA), *Pseudomonas aeruginosa*, *Acinetobacter baumannii*, three different strains of *Mtb* (reference H37RV, and isolated isoniazid resistant (INH) and susceptible strains), *Mycobacterium terrae and Mycobacterium avium* (Tables 2 and 3). Polycations C0-T-p, C8-T-p, C0-D-p, and C8-D-p were chosen as representative examples of hydrophilic/hydrophobic and flexible/rigid molecules.

The highly hydrophobic C8-D-p and C8-T-p showed no activity against non-*Mycobacterium* clinical strains within the tested concentration range, in contrast to the relatively

Table 2 Activity against clinically isolated strains

	MIC [μg mL^{-1}]					
	Gram-negative bacteria				Gram-positive bacteria	
Polymer	*K. pneumoniae*[a] (MBL, NDM type)	*K. pneumoniae*[a] (ESBL)	*P. aeruginosa*[a]	*A. baumannii*[a]	*S.aureus*[b] (MRSA)	*E. faecium*[b] (VRE)
C0-D-p	512	256	>512	>512	32	>512
C0-T-p	64	128	64	64	32	16
C8-D-p	>512	>512	>512	>512	>512	>512
C8-T-p	>512	>512	>512	>512	>512	>512
CIP[c]	>64	64	>64	>64	>64	>64

[a] Gram-negative bacteria. [b] Gram-positive bacteria. [c] Ciprofloxacin (CIP).

Table 3 Activity against *Mycobacterium* species

	MIC [μg mL^{-1}]				
Polymer	*M. tuberculosis* H37RV	*M. tuberculosis* 210 (INH resistant)	*M. tuberculosis* 192 (INH susceptible)	*M. terrae*	*M. avium*
C0-D-p	32	64	64	16	512
C0-T-p	16	16	32	8	256
C8-D-p	16	16	32	32	>512
C8-T-p	16	16	32	8	>512
INH[a]	≤0.0625	2	≤0.0625	64	64
RMP[b]	0.5	16	0.5	4	32

[a] Isoniazid. [b] Rifampicin.

hydrophilic C0-D-p and C0-T-p (Table 2). The rigid C0-D-p is moderately active against MRSA only, and displays limited activity against both *K. pneumoniae* strains. In contrast, the flexible C0-T-p is moderately active against all tested pathogens. In these studies, ciprofloxacin (CIP) was applied as a benchmark because both CIP and C0-ionenes show bactericidal rather than bacteriostatic activity.[53] C0-T-p shows lower MICs than CIP for the majority of the tested isolates. Activity against MRSA (MIC 32 μg mL^{-1}; Table 2) is significantly lower than against the model *S. aureus* from the ATCC collection (MIC 2–4 μg mL^{-1}; Fig. 3a). The difference between MRSA and the model *S. aureus* strains lays in the structure of the penicillin-binding proteins (PBP).[67] However, this feature is unlikely to induce the observed increase in the MICs. Some other structural features, *e.g.*, a different cell membrane composition, may be responsible for the lower susceptibility of MRSA to ionenes. The structure–activity relationship observed for model microorganisms, namely, the lower antibacterial potency of the more hydrophobic and conformationally constrained ionenes, also applies to the pathogenic strains.

Both tested C8 ionenes and C0-T-p are comparably active toward *Mtb*, whereas C0-D-p is weaker (Table 3). When the activity toward *M. terrae* is considered, a higher activity of the flexible TMEDA-containing ionenes than that of the more rigid ones may be noticed. Two of the tested ionenes show very weak activity toward *M. avium*.

The hydrophobic modification of polymers, in the form of the C8 alkyl group, does not lower the ionene activity against mycobacteria (Table 3). The comparison between the MICs values of C0-D-p and C0-T-p against all studied mycobacteria indicates a higher activity of the flexible ionenes. A different response of mycobacteria to the presence of alkyl hydrophobic side chains, in comparison to all of the other tested microorganisms, can be associated with the cell envelope structure. *Mycobacterium* has a complex thick cell wall consisting of peptidoglycan, arabinogalactan, and hydrophobic mycolic acids covered by mycolates, phospholipids, and lipoglycans, whereas the cell walls of Gram-positive and Gram-negative bacteria predominantly consist of peptidoglycan.[39] No HLB influence on antimycobacterial activity was observed for the discussed ionenes. However, other published studies provide rather inconclusive results in this respect. For example, in our previous paper, we observed an increase of such activity when the hydrophobicity of the polyethyleneimine derivatives was increased.[48] On the other hand, P. Yavvari observed the opposite trend for poly-aspartamide derivatives.[47] Ionenes C8-T-p and C8-D-p showed high selectivity toward mycobacteria over other tested clinical isolates. Such selectivity of polycations was also reported previously for the alkylated dimethyl-aminopropyl poly-aspartamides,[47] poly(dimethylaminoethyl) methacrylate,[46] and cationic phosphorus dendrimers.[42] Activity against *Mtb*, for the discussed herein polymers, remains at similar levels to the

previously reported ionenes (MIC values 2–40 μg mL^{-1}).[33,42,45,47,48] For example, an ionene with a structure similar to C0-T-p, studied by J. Tan *et al.*, displayed a MIC value of 16 μg mL^{-1} against different *Mtb* strains.[33]

3.2.6 Killing kinetics of model bacteria. The observed impact of the main-chain flexibility and overall hydrophobicity on the growth inhibitory activity raised the question of whether those parameters also affect the bactericidal activity of ionenes and their killing rate. To answer such question, C0-T-p, C0-D-p, C8-T-p, and C8-D-p ionenes were used in time-killing assays against *E. coli* and *S. aureus* from ATCC. Selected polycations were tested at concentrations equal to their multiple MIC values (1, 2, 4 × MIC).

Ionenes C0-T-p, C8-T-p, and C8-D-p exert bacteriostatic activity against *S. aureus* since they do not reduce colony-forming units (CFU) during 1 h incubation at the concentration of 1 × MIC (Fig. 4a, c and d). Only C0-D-p shows bactericidal activity at 1 × MIC, reducing the initial CFU by 95% after 60 min of incubation (Fig. 4b). At the concentration of 2× MIC, ionenes C0-T-p and C0-D-p kill more than 99.9% of bacteria in the sample after 5 min incubation (Fig. 4a and b). In contrast, their more hydrophobic analogs, containing the C8 group, work significantly slower. After 60 min of incubation, CFU was reduced to almost 0.1% of its initial value (Fig. 4c and d). These hydrophobic ionenes require the concentration of 4 × MIC to eradicate all *S. aureus* from the sample.

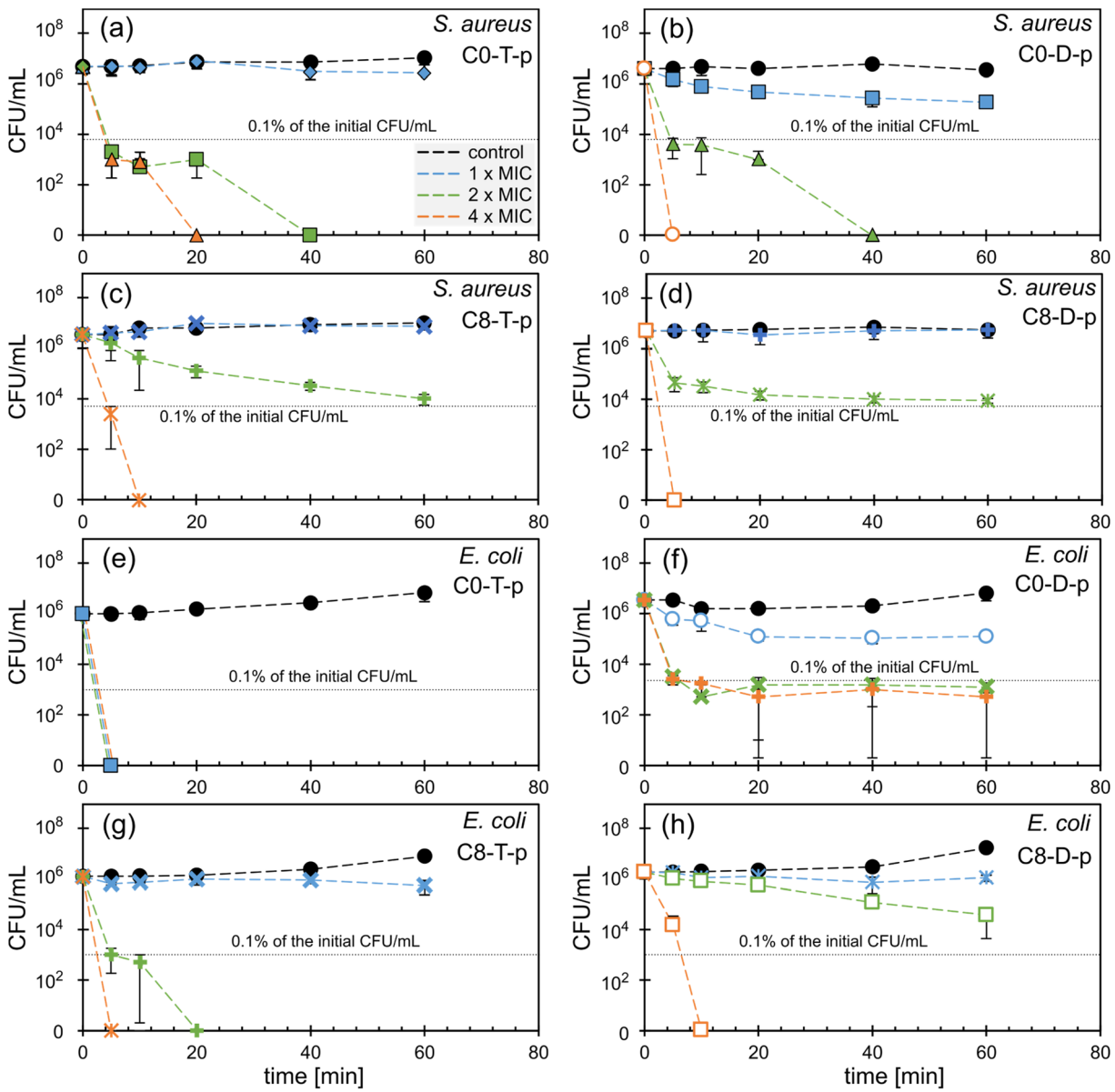

Fig. 4 The killing-kinetic of (a–d) *E. coli* (ATCC 8739) and (e–h) *S. aureus* (ATCC 6538) by (a and e) C0-T-p, (b and f) C0-D-p, (c and g) C8-T-p, and (d and h) C8-D-p. The legend on (a) applies the entire figure; the symbols are related to the ionenes concentration: (●) 0 μg mL^{-1}, (◆) 2 μg mL^{-1}, (■) 4 μg mL^{-1}, (▲) 8 μg mL^{-1}, (○) 16 μg mL^{-1}, (×) 32 μg mL^{-1}, (+) 64 μg mL^{-1}, (✱) 128 μg mL^{-1}, (□) ≥256 μg mL^{-1}.

Polymer C0-T-p shows the highest effectiveness against *E. coli*, killing all bacteria at the concentration of 1 × MIC (4 μg mL^{-1}) after just 5 min of incubation (Fig. 4e). The less flexible analog, C0-D-p, also reduces the initial CFU by 97% after 60 min at the concentration of 1 × MIC (16 μg mL^{-1}). However, at 2 and 4 × MIC, the reduction reaches 99.9% after 5 min (Fig. 4f). In contrast to the C0 polymers, C8 derivatives show bacteriostatic activity only at the concentration of 1 × MIC (Fig. 4g and h). The more flexible C8-T-p eliminates all bacteria at 2 × MIC, whereas the stiff C8-D-p requires as much as 4 × MIC to get a similar effect within the studied time range.

All tested C0 ionenes displayed higher killing rates than their hydrophobic C8 analogs. C0-T-p is particularly active with clear bactericidal activity at a concentration of 4 μg mL^{-1} and MBC close to MIC values. Considering the influence of the main-chain flexibility, one may notice that this parameter does not significantly impact activity toward *S. aureus*. However, the more flexible TMEDA-containing ionenes exert stronger and faster bactericidal potency toward *E. coli* than their rigid analogs. Flexibility of the main chain affects the killing efficiency and bacteria growth inhibition for both *S. aureus* and *E. coli* in a similar way (Fig. 3). This effect is much more pronounced for *E. coli* than *S. aureus*. The fast killing kinetics of the presented ionenes prove their contact mechanism of action, which was previously investigated for this class of polycations in other works.[36,53,54]

4. Conclusions

The comparison of the MIC values against the model microorganisms determined for the ionenes obtained in this work (C*n*-T-m and C*n*-D-p series), and for previously published compounds (C*n*-T-p[53] and C*n*-D-m[54] series), allowed us to discuss the cross-influence of hydrophobicity, mainchain flexibility, and topology on the antimicrobial activity. The topology, resulting from different isomers of the aryl linker and located within the polymeric main-chain, seems not to affect the growth inhibitory activity, whereas the increased hydrophilicity and main-chain flexibility increases the antimicrobial activity. The elevated hydrophobicity also increases toxicity against red blood cells. The impact of these parameters is clearly visible in the case of *C. albicans* and *E. coli*, and less against *S. aureus*. Killing kinetics studies showed that strongly hydrophobic C8 ionenes are less bactericidal against both tested bacteria than their more hydrophilic C0 analogs, whereas the main-chain stiffness affects the killing rate against *E. coli* only. Further studies on selected ionenes revealed good activity toward drug resistance clinical isolates, and confirmed that the polymeric chain flexibility of ionenes should be considered besides their hydrophobicity to obtain more potent antimicrobial agents.

The studied ionenes show good activity toward mycobacteria species, including *Mtb*, which is an important result in light of the returning tuberculosis disease threat. Interestingly, in contrast to other tested microorganisms, the excessive hydrophobicity of ionenes does not affect the potency of the polycations toward mycobacteria. It indicates that the polycations developed against *Mycobacteria* require a unique HLB, which should be separately optimized. Data gathered on the clinical strains and bactericidal kinetics experiments confirmed that C0-T-p is the most active and promising structure in the investigated library.

Conflicts of interest

The authors declare no conflict of interest.

Acknowledgements

This work was financially supported by the National Science Center, Poland (PoCoDi project, grant 2015/18/E/ST5/00222), and by the Faculty of Chemistry, Warsaw University of Technology.

References

1 *Antibacterial agents in clinical development: an analysis of the antibacterial clinical development pipeline*, World Health Organization, Geneva, 2019, Licence: CC BY-NC-SA 3.0 IGO.
2 J. J. De Waele, M. Akova, M. Antonelli, R. Canton, J. Carlet, D. De Backer, G. Dimopoulos, J. Garnacho-Montero, J. Kesecioglu, J. Lipman, M. Mer, J. A. Paiva, M. Poljak, J. A. Roberts, J. Rodriguez Bano, J. F. Timsit, J. R. Zahar and M. Bassetti, *Intensive Care Med.*, 2018, **44**, 189–196.
3 J. Chakaya, M. Khan, F. Ntoumi, E. Aklillu, R. Fatima, P. Mwaba, N. Kapata, S. Mfinanga, S. E. Hasnain, P. D. M. C. Katoto, A. N. H. Bulabula, N. A. Sam-Agudu, J. B. Nachega, S. Tiberi, T. D. McHugh, I. Abubakar and A. Zumla, *Int. J. Infect. Dis.*, 2021, **113**, S7–S12.
4 *Global tuberculosis report 2020*, World Health Organization, 2020, Geneva, Licence: CC BY-NC-SA 3.0.
5 M. Lakemeyer, W. Zhao, F. A. Mandl, P. Hammann and S. A. Sieber, *Angew. Chem., Int. Ed.*, 2018, **57**, 14440–14475.
6 B. Spellberg, R. Guidos, D. Gilbert, J. Bradley, H. W. Boucher, W. M. Scheld, J. G. Bartlett and J. Edwards, *Clin. Infect. Dis.*, 2008, **46**, 155–164.
7 C. Nathan and O. Cars, *N. Engl. J. Med.*, 2014, **371**, 1761–1763.
8 L. J. V. Piddock, *Lancet Infect. Dis.*, 2012, **12**, 249–253.
9 H. Wang, M. Niu, T. Xue, L. Ma, X. Gu, G. Wei, F. Li and C. Wang, *J. Mater. Chem. B*, 2022, **10**, 1858–1874.
10 O. Stachurski, D. Neubauer, I. Małuch, D. Wyrzykowski, M. Bauer, S. Bartoszewska, W. Kamysz and E. Sikorska, *Bioorg. Med. Chem.*, 2019, **27**, 115129.
11 Y. Yuan, F. Zhou, H. Su and Y. Zhang, *Sci. Rep.*, 2019, **9**, 11885.
12 Y. Yuan, S. Liang, J. Li, S. Zhang and Y. Zhang, *J. Mater. Chem. B*, 2019, **7**, 5620–5625.
13 N. Wiradharma, M. Khan, L.-K. Yong, C. A. E. Hauser, S. V. Seow, S. Zhang and Y.-Y. Yang, *Biomaterials*, 2011, **32**, 9100–9108.
14 M. S. Ganewatta and C. Tang, *Polymer*, 2015, **63**, A1–A29.
15 C. Ergene, K. Yasuhara and E. F. Palermo, *Polym. Chem.*, 2018, **9**, 2407–2427.
16 Y. Yang, Z. Cai, Z. Huang, X. Tang and X. Zhang, *Polym. J.*, 2018, **50**, 33–44.

17 S.-B. T. A. Amos, L. S. Vermeer, P. M. Ferguson, J. Kozlowska, M. Davy, T. T. Bui, A. F. Drake, C. D. Lorenz and A. J. Mason, *Sci. Rep.*, 2016, **6**, 37639.
18 L. Liu, Y. Fang and J. Wu, *Biochim. Biophys. Acta, Biomembr.*, 2013, **1828**, 2479–2486.
19 A. Oddo, T. T. Thomsen, H. M. Britt, A. Løbner-Olesen, P. W. Thulstrup, J. M. Sanderson and P. R. Hansen, *ACS Med. Chem. Lett.*, 2016, **7**, 741–745.
20 T. Ronček, D. Vukičević, N. Ilić, L. Krce, G. Gajski, M. Tonkić, I. Goić-Barišić, L. Zoranić, Y. Sonavane, M. Benincasa, D. Juretić, A. Maravić and A. Tossi, *J. Med. Chem.*, 2018, **61**, 2924–2936.
21 J. Bachl, O. Bertran, J. Mayr, C. Alemán and D. Díaz Díaz, *Soft Matter*, 2017, **13**, 3031–3041.
22 M. Häring, S. Grijalvo, D. Haldar, C. Saldías and D. D. Díaz, *Eur. Polym. J.*, 2019, **115**, 221–224.
23 M. G. Saborío, O. Bertran, S. Lanzalaco, M. Häring, L. Franco, J. Puiggalí, D. D. Díaz, F. Estrany and C. Alemán, *Soft Matter*, 2018, **14**, 6374–6385.
24 V. Sambhy, B. R. Peterson and A. Sen, *Angew. Chem., Int. Ed.*, 2008, **47**, 1250–1254.
25 T. Eren, A. Som, J. R. Rennie, C. F. Nelson, Y. Urgina, K. Nüsslein, E. B. Coughlin and G. N. Tew, *Macromol. Chem. Phys.*, 2008, **209**, 516–524.
26 W. Chin, C. Yang, V. W. L. Ng, Y. Huang, J. Cheng, Y. W. Tong, D. J. Coady, W. Fan, J. L. Hedrick and Y. Y. Yang, *Macromolecules*, 2013, **46**, 8797–8807.
27 D. S. S. M. Uppu, S. Samaddar, J. Hoque, M. M. Konai, P. Krishnamoorthy, B. R. Shome and J. Haldar, *Biomacromolecules*, 2016, **17**, 3094–3102.
28 E. F. Palermo and K. Kuroda, *Biomacromolecules*, 2009, **10**, 1416–1428.
29 C. Ergene and E. F. Palermo, *J. Mater. Chem. B*, 2018, **6**, 7217–7229.
30 K. You, B. Gao, M. Wang, X. Wang, K. C. Okoro, A. Rakhimbekzoda and Y. Feng, *J. Mater. Chem. B*, 2022, **10**, 1005–1018.
31 R. J. Kopiasz, W. Tomaszewski, A. Kuźmińska, K. Chreptowicz, J. Mierzejewska, T. Ciach and D. Jańczewski, *Macromol. Biosci.*, 2020, **20**, 2000063.
32 C. Krumm, S. Trump, L. Benski, J. Wilken, F. Oberhaus, M. Köller and J. C. Tiller, *ACS Appl. Mater. Interfaces*, 2020, **12**, 21201–21209.
33 J. P. K. Tan, J. Tan, N. Park, K. Xu, E. D. Chan, C. Yang, V. A. Piunova, Z. Ji, A. Lim, J. Shao, A. Bai, X. Bai, D. Mantione, H. Sardon, Y. Y. Yang and J. L. Hedrick, *Macromolecules*, 2019, **52**, 7878–7885.
34 S. Venkataraman, J. P. K. Tan, S. T. Chong, C. Y. H. Chu, E. A. Wilianto, C. X. Cheng and Y. Y. Yang, *Biomacromolecules*, 2019, **20**, 2737–2742.
35 W. Lou, S. Venkataraman, G. Zhong, B. Ding, J. P. K. Tan, L. Xu, W. Fan and Y. Y. Yang, *Acta Biomater.*, 2018, **78**, 78–88.
36 S. Liu, R. J. Ono, H. Wu, J. Y. Teo, Z. C. Liang, K. Xu, M. Zhang, G. Zhong, J. P. K. Tan, M. Ng, C. Yang, J. Chan, Z. Ji, C. Bao, K. Kumar, S. Gao, A. Lee, M. Fevre, H. Dong, J. Y. Ying, L. Li, W. Fan, J. L. Hedrick and Y. Y. Yang, *Biomaterials*, 2017, **127**, 36–48.
37 S. Bai, J. Wang, K. Yang, C. Zhou, Y. Xu, J. Song, Y. Gu, Z. Chen, M. Wang, C. Shoen, B. Andrade, M. Cynamon, K. Zhou, H. Wang, Q. Cai, E. Oldfield, S. C. Zimmerman, Y. Bai and X. Feng, *Sci. Adv.*, 2021, **7**, 1–17.
38 Z. Chen, C. Zhou, Y. Xu, K. Wen, J. Song, S. Bai, C. Wu, W. Huang, Q. Cai, K. Zhou, H. Wang, Y. Wang, X. Feng and Y. Bai, *Biomaterials*, 2021, **275**, 120858.
39 H. Chen, S. A. Nyantakyi, M. Li, P. Gopal, D. B. Aziz, T. Yang, W. Moreira, M. Gengenbacher, T. Dick and M. L. Go, *Front. Microbiol.*, 2018, **9**, 1627.
40 P. J. Brennan, *Tuberculosis*, 2003, **83**, 91–97.
41 S. Bansal, M. Singh, S. Kidwai, P. Bhargava, A. Singh, V. Sreekanth, R. Singh and A. Bajaj, *MedChemComm*, 2014, **5**, 1761–1768.
42 S. Mignani, V. D. Tripathi, D. Soam, R. P. Tripathi, S. Das, S. Singh, R. Gandikota, R. Laurent, A. Karpus, A.-M. Caminade, A. Steinmetz, A. Dasgupta, K. K. Srivastava and J.-P. Majoral, *Biomacromolecules*, 2021, **22**, 2659–2675.
43 A. W. Simonson, A. S. Mongia, M. R. Aronson, J. N. Alumasa, D. C. Chan, A. Lawanprasert, M. D. Howe, A. Bolotsky, T. K. Mal, C. George, A. Ebrahimi, A. D. Baughn, E. A. Proctor, K. C. Keiler and S. H. Medina, *Nat. Biomed. Eng.*, 2021, **5**, 467–480.
44 S. Ramón-García, R. Mikut, C. Ng, S. Ruden, R. Volkmer, M. Reischl, K. Hilpert and C. J. Thompson, *Antimicrob. Agents Chemother.*, 2013, **57**, 2295–2303.
45 L. M. Timofeeva, N. A. Kleshcheva, M. O. Shleeva, M. P. Filatova, Y. A. Simonova, Y. A. Ermakov and A. S. Kaprelyants, *Appl. Microbiol. Biotechnol.*, 2015, **99**, 2557–2571.
46 D. J. Phillips, J. Harrison, S.-J. Richards, D. E. Mitchell, E. Tichauer, A. T. M. Hubbard, C. Guy, I. Hands-Portman, E. Fullam and M. I. Gibson, *Biomacromolecules*, 2017, **18**, 1592–1599.
47 P. S. Yavvari, S. Gupta, D. Arora, V. K. Nandicoori, A. Srivastava and A. Bajaj, *Biomacromolecules*, 2017, **18**, 2024–2033.
48 D. Kozon, J. Mierzejewska, T. Kobiela, A. Grochowska, K. Dudnyk, A. Głogowska, A. Sobiepanek, A. Kuźmińska, T. Ciach, E. Augustynowicz-Kopeć and D. Jańczewski, *Macromol. Biosci.*, 2019, **19**, 1900254.
49 S.-J. Richards, K. Isufi, L. E. Wilkins, J. Lipecki, E. Fullam and M. I. Gibson, *Biomacromolecules*, 2018, **19**, 256–264.
50 M. U. Shiloh and P. A. DiGiuseppe Champion, *Curr. Opin. Microbiol.*, 2010, **13**, 86–92.
51 N. Lelovic, K. Mitachi, J. Yang, M. R. Lemieux, Y. Ji and M. Kurosu, *J. Antibiot.*, 2020, **73**, 780–789.
52 A. Sharma, A. A. Pohane, S. Bansal, A. Bajaj, V. Jain and A. Srivastava, *Chem.–Eur. J.*, 2015, **21**, 3540–3545.
53 R. J. Kopiasz, A. Rukasz, K. Chreptowicz, R. Podgórski, A. Kuźmińska, J. Mierzejewska, W. Tomaszewski, T. Ciach and D. Jańczewski, *Colloids Surf., B*, 2021, **207**, 112016.
54 R. J. Kopiasz, N. Kulbacka, K. Drężek, R. Podgórski, I. Łojszczyk, J. Mierzejewska, T. Ciach, E. Augustynowicz-Kopeć, A. Głogowska, A. Iwańska, W. Tomaszewski and D. Jańczewski, *Macromol. Biosci.*, 2022, 2200094.

55 J. M. Layman, E. M. Borgerding, S. R. Williams, W. H. Heath and T. E. Long, *Macromolecules*, 2008, **41**, 4635–4641.
56 J. Aguiar, P. Carpena, J. A. Molina-Bolívar and C. Carnero Ruiz, *J. Colloid Interface Sci.*, 2003, **258**, 116–122.
57 A. Strassburg, F. Kracke, J. Wenners, A. Jemeljanova, J. Kuepper, H. Petersen and J. C. Tiller, *Macromol. Biosci.*, 2015, **15**, 1710–1723.
58 M. S. Ganewatta, M. A. Rahman, L. Mercado, T. Shokfai, A. W. Decho, T. M. Reineke and C. Tang, *Bioact. Mater.*, 2018, **3**, 186–193.
59 K. E. S. Locock, T. D. Michl, J. D. P. Valentin, K. Vasilev, J. D. Hayball, Y. Qu, A. Traven, H. J. Griesser, L. Meagher and M. Haeussler, *Biomacromolecules*, 2013, **14**, 4021–4031.
60 R. Liu, X. Chen, S. Chakraborty, J. J. Lemke, Z. Hayouka, C. Chow, R. A. Welch, B. Weisblum, K. S. Masters and S. H. Gellman, *J. Am. Chem. Soc.*, 2014, **136**, 4410–4418.
61 N. A. R. Gow and B. Hube, *Curr. Opin. Microbiol.*, 2012, **15**, 406–412.
62 N. Malanovic and K. Lohner, *Biochim. Biophys. Acta, Biomembr.*, 2016, **1858**, 936–946.
63 E. F. Palermo, K. Lienkamp, E. R. Gillies and P. J. Ragogna, *Angew. Chem., Int. Ed.*, 2019, **58**, 3690–3693.
64 G. J. Gabriel, J. A. Maegerlein, C. F. Nelson, J. M. Dabkowski, T. Eren, K. Nüsslein and G. N. Tew, *Chem.–Eur. J.*, 2009, **15**, 433–439.
65 J. Mayr, J. Bachl, J. Schlossmann and D. D. Díaz, *Int. J. Mol. Sci.*, 2017, **18**, 303.
66 S. N. Riduan, Y. Yuan, F. Zhou, J. Leong, H. Su and Y. Zhang, *Small*, 2016, **12**, 1928–1934.
67 P. D. Stapleton and P. W. Taylor, *Sci. Prog.*, 2002, **85**, 57–72.